

TWO-NUCLEON SCATTERING BY A CENTRAL POTENTIAL

Asset Kabdiyev and Nicolas Dronchi

1 Introduction

Scattering processes are a crucial part of today's physical research. They are a primary way in which we learn experimentally about distributions in mass, charge, and, in general potential energy for molecular, atomic, and subatomic system. In this project we will examine two-nucleon scattering by a central potential, for which the potential is $-V_0$ for $r < R$, and zero for $r > R$. In order to do this we will simulate in Python mathematical model of the scattering and derive the scattering cross section from a quantum mechanical point of view. For the numerically solution of the radial equation will be used Numerov's algorithm. The results will give us an insight into the dependence of scattering cross sections on different parameters such as energy and angular momentum of the wave. The final point of our project will be validating of numerical solution in S-wave with the analytical solution of the phase shift and the cross section.

2 Research methodology and background

2.1 Schrödinger equation and Numerov's method

An essential part of the derivation of scattering cross sections involves the solution of the Schrödinger equation for central potential.

$$-\frac{\hbar^2}{2\mu}u''(r) + [V(r) + \frac{\hbar^2}{2\mu} \frac{\ell(\ell+1)}{r^2}] u(r) = E u(r), \quad (1)$$

where

$$E = \frac{\hbar^2 k^2}{2\mu}, \quad \text{and} \quad \mu = \frac{m}{2}. \quad (2)$$

We will use the Numerov's algorithm to numerically solve this equation. We define

$$v(r) = \frac{2\mu}{\hbar^2} V(r) = \frac{938 \text{ Mev}}{\sim 197 \text{ Mev fm}}, \quad (3)$$

and rewrite the equation above as

$$u''(r) + \left[k^2 - v(r) - \frac{\ell(\ell+1)}{r^2} \right] u(r) = 0, \quad (4)$$

or

$$u''(r) + K(r)u(r) = 0, \quad (5)$$

with

$$K(r) = \frac{2\mu}{\hbar^2} [E - V(r)] - \frac{\ell(\ell+1)}{r^2}. \quad (6)$$

As $r \rightarrow 0$, $u(r) \rightarrow r^{(\ell+1)}$. We use two grid points close to zero (*e.g.*, $r_1 = h$ and $r_2 = 2 \times h$, where h is the step in r), and the solution calculated in these points, that is

$u_1 = u(r_1) = h^{\ell+1}$ and $u_2 = u(r_2) = (2 \times h)^{\ell+1}$, to start building the solution outwards using the Numerov's method. The subsequent u_i 's calculated at r_i 's are obtained using the following algorithm taken out to some R_{max}

$$u_{i+1} \left(1 + \frac{h^2}{12} K_{i+1} \right) - u_i \left(2 - \frac{5h^2}{6} K_i \right) + u_{i-1} \left(1 + \frac{h^2}{12} K_{i-1} \right) + O(h^6) = 0.$$

2.2 Partial wave expansion and scattering cross section

Once again let's look at the Schrödinger equation for central potential (1)

$$-\frac{\hbar^2}{2\mu} u''(r) + [V(r) + \frac{\hbar^2}{2\mu} \frac{\ell(\ell+1)}{r^2}] u(r) = E u(r),$$

The wave function $\Phi_{out}(r)$ describes the neutron, so it must be a superposition of the incoming and the outgoing wave in the asymptotic form

$$\Phi_{out}(r) = \exp(i\mathbf{k} \cdot \mathbf{r}) + \frac{\exp(ikr)}{r} f_k(\theta), \quad (7)$$

The reason an asymptotic form of the wave function is used, is that the observer is far away compared to the size of the neutrons ($r \Rightarrow \infty$) and is therefore in the asymptotic region. Then we will expand wave function in eigenstates of the orbital angular momentum

$$\exp(i\mathbf{k} \cdot \mathbf{r}) = \sum_{k=1}^{\infty} i^l (2l+1) j_l(kr) P_l(\cos \theta), \quad (8)$$

We can similarly expand

$$f_k(\theta) = \sum_{k=1}^{\infty} i^l (2l+1) f_l(k) P_l(\cos \theta), \quad (9)$$

Where f_l is the partial wave amplitude. It can be represented as

$$f_l(k) = \frac{\exp(i\delta_l)}{k} \sin(\delta_l), \quad (10)$$

Assuming only radial direction ($\theta = 0$) we can substitute f_k in the cross section formula

$$\frac{d\sigma}{d\Omega} = |f_k(\theta)|^2 \Rightarrow \sigma = \int d\sigma |f_k(\theta)|^2, \quad (11)$$

Finally we get

$$\sigma = 4\pi \sum_{l=0}^{\infty} (2l+1) |f_l(k)|^2, \quad (12)$$

or

$$\sigma = 4 \frac{\pi}{k^2} \sum_{l=0}^{\infty} (2l+1) \sin^2(\delta_l). \quad (13)$$

2.3 Scattering phase shift

To completely derive the differential and the total cross section we need to find equation for scattering phase shift. By tradition we start our calculations with the Schödinger equation (1)

$$-\frac{\hbar^2}{2\mu}u''(r) + [V(r) + \frac{\hbar^2}{2\mu} \frac{\ell(\ell+1)}{r^2}]u(r) = E u(r),$$

If we replace

$$u(r) = rR(r), \quad (14)$$

We can get the solution for the outside region

$$R_l^>(r) = C_1 h_1(kr) + C_2 h_2(kr), \quad (15)$$

Where h_1, h_2 are Haukel functions and for boundary condition $kr \Rightarrow \infty$

$$h_1, h_2 = \pm \frac{\exp(\pm i(kr - l\frac{\pi}{2}))}{ikr}, \quad (16)$$

By expanding wave function in eigenstates of the orbital angular momentum we can obtain

$$\Phi^>(r) = \sum_{k=1}^{\infty} i^l (2l+1) P_l(\cos \theta) \times R_l^>(r), \quad (17)$$

And comparing of $\Phi^>(r)$ with $\Phi_{out}(r)$, which was obtained by solving equations (2.8)-(2.11), gives us coefficients C_l^1 and C_l^2

$$C_l^1 = \frac{\exp(2i\delta_l)}{2}, \quad C_l^2 = \frac{1}{2}. \quad (18)$$

All this equations lead us to the final solution for the outside region

$$R_l^>(r) = \exp(i\delta_l)[\cos(\delta_l)j_l(kr) - \sin(\delta_l)n_l(kr)], \quad (19)$$

Where $j_l(kr)$ is the Bessel function and $n_l(kr)$ is the Neumann function. From here, to numerically get the phase shift, we take the ratio of $R_l^>(r)$ at two points far from the origin. In this case it is convenient to take $r_1 = R_{max} - h$ and $r_2 = R_{max}$

$$\frac{R_l(r_1)}{R_l(r_2)} = \frac{\cos(\delta_l)j_l(kr_1) - \sin(\delta_l)n_l(kr_1)}{\cos(\delta_l)j_l(kr_2) - \sin(\delta_l)n_l(kr_2)}, \quad (20)$$

Substituting in α where

$$\alpha = \frac{R_l(r_1)}{R_l(r_2)} = \frac{u(r_1)}{r_1} \frac{r_2}{u(r_2)}, \quad (21)$$

we can invert to solve for the phase shift so that the following is convenient for numerically calculating the phase shift

$$\tan(\delta_l) = \frac{j_l(kr_1) - \alpha j_l(kr_2)}{n_l(kr_1) - \alpha n_l(kr_2)}, \quad (22)$$

2.4 Analytical solution

The traditional method of validating a simulation is to identify a problem that is simple enough that an analytical or closed form solution exists. The main goal of our project is to find two nucleon scattering by square potential well, for which the potential is $-V_0$ for $r < R$, and zero for $r > R$. We can simplify this problem and solve it analytically by considering only S-wave scattering ($l = 0$). Then we can compare a numerically computed

solution with the analytically known true result.

First, by setting ($l = 0$) we can obtain

$$j_0(x) = \frac{\sin(x)}{x}, n_0(x) = \frac{-\cos(x)}{x}, \quad (23)$$

When considering this in equation (19) we get the solution for the outside region

$$R_l^>(r) = \exp(i\delta_0) \sin(kr + \delta_0). \quad (24)$$

For the inside region we use Schrödinger equation (5) with

$$K(r) = \frac{2\mu}{\hbar^2} [E - V(r_0)], \quad (25)$$

With general solution

$$u_0^<(r) = A \frac{\sin(Kr)}{Kr}. \quad (26)$$

Continuity of the wave function at point $r = R$

$$u_0^<(r)|_{r=R} = u_0^>(r)|_{r=R}, \quad (27)$$

Leads us

$$A = \frac{K}{k} \exp(i\delta_0) \frac{\sin(kR + \delta_0)}{\sin(KR)}, \quad (28)$$

Also we know that the first derivative of the wave function should be continuous

$$R_0^<(r)|_{r=R} = R_0^>(r)|_{r=R}, \quad (29)$$

so

$$A \cos(KR) = \exp(i\delta_0) \cos(kR + \delta_0). \quad (30)$$

Substitution of A by the equation (28) yields

$$\tan(kR + \delta_0) = \frac{k}{K} \frac{\sin(KR)}{\cos(KR)}, \quad (31)$$

We can rewrite the equation above as

$$\tan(\delta_0) = \frac{\cos(kR) \sin(KR) - \frac{K}{k} \cos(KR) \sin(kR)}{\frac{K}{k} \cos(kR) \cos(KR) + \sin(kR) \sin(KR)}, \quad (32)$$

And finally

$$\delta_0 = \arctan \frac{\cos(kR) \sin(KR) - \frac{K}{k} \cos(KR) \sin(kR)}{\frac{K}{k} \cos(kR) \cos(KR) + \sin(kR) \sin(KR)}. \quad (33)$$

Cross section can be obtained by the equation (13) with $l = 0$. This analytical solution of the phase shift and the cross section in S-wave will be used to validate our code.

3 Results and Analysis

3.1 Wave functions

Here the results of the numerical solutions are shown. Using Numerov's algorithm discussed in the methods, the wave function solutions to Schrodinger's equations were calculated. Keeping the waves as functions radial wave functions $U(r)$, related to $R(r)$ through equation (14). The wave functions for the S, P, and D-waves are plotted at energies of 1, 10, 100, and 200 in figure 1 for a central potential depth of 20 MeV. For a central potential depth of 60 MeV, see figure 2.

Seen most clearly in the difference between figure 1(a) and figure 2(a), the wave functions must match inner and outer wave functions at the boundary of the potential at $R = 1.45$ fm.

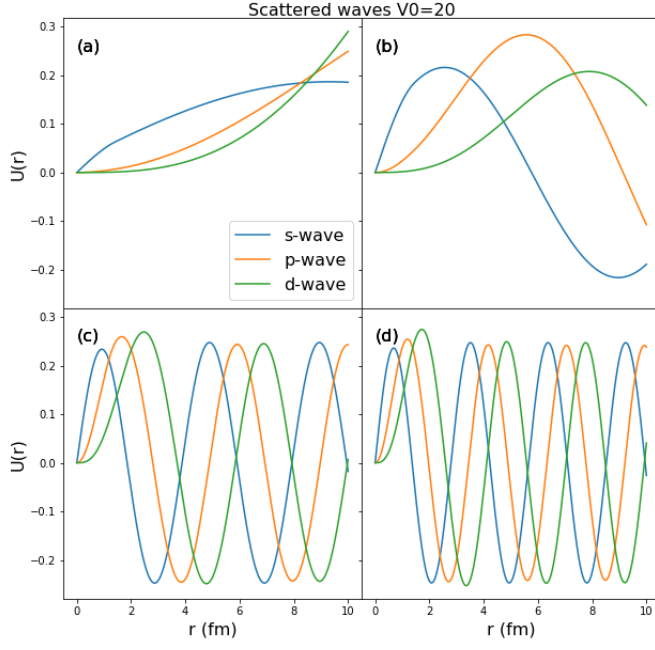


Figure 1: Radial wavefunctions of S, P, and D waves (a) Incoming nucleon at 1 MeV, (b) incoming nucleon at 10 MeV, (c) incoming nucleon at 100 MeV, and (d) incoming nucleon at 200 MeV. The potential depth was set to 20 MeV

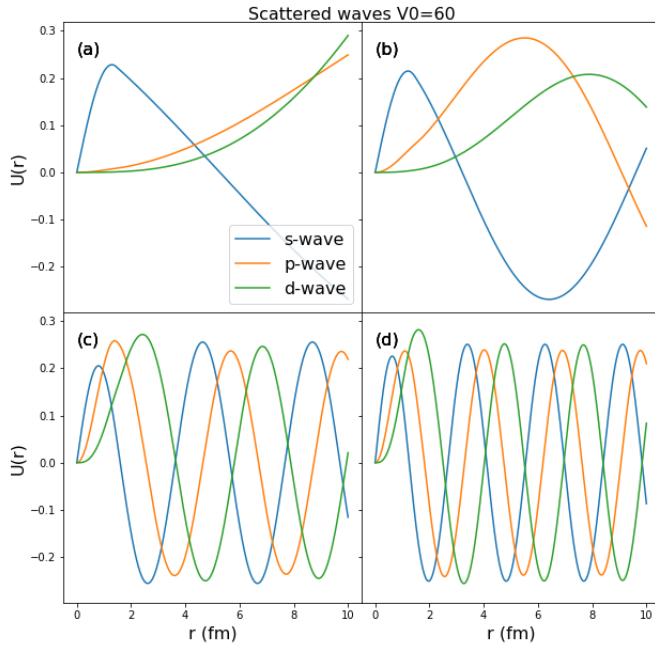


Figure 2: Radial wavefunctions of S, P, and D waves (a) Incoming nucleon at 1 MeV, (b) incoming nucleon at 10 MeV, (c) incoming nucleon at 100 MeV, and (d) incoming nucleon at 200 MeV. The potential depth was set to 60 MeV

3.2 Phase Shifts and Cross Sections

The phase shifts were numerically calculated with the description seen in equation 22. To validate the numerical calculation, an analytical solution to the S-wave phase shifts can be found in the form of equation 33. Here, the S-wave phase shifts are plotted in figure 3 as a function of energy. There is a strong agreement in low and high energy phase shifts.

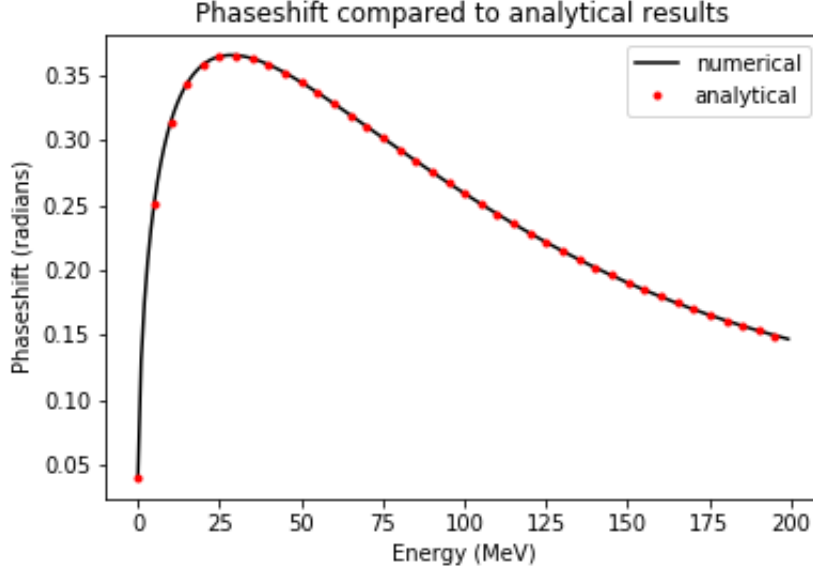


Figure 3: Numerical and analytical phase shifts plotted as a function of energy for a potential depth of 20 MeV

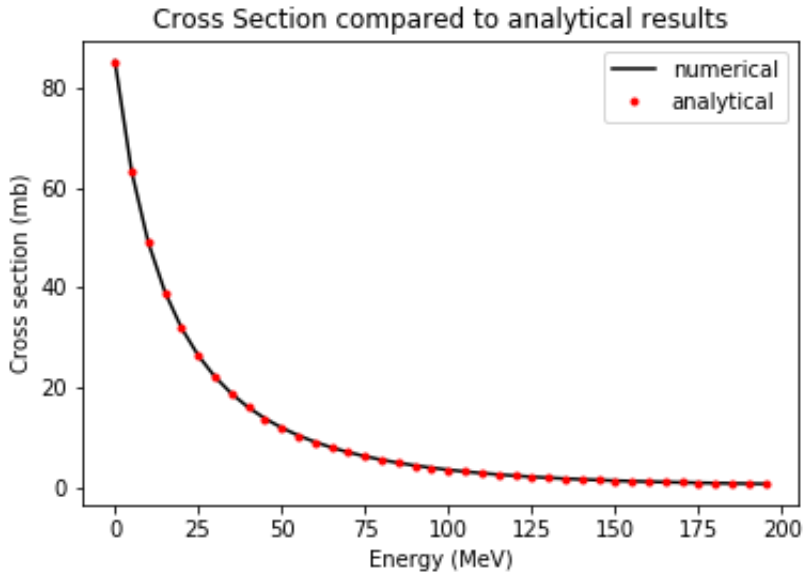


Figure 4: Numerical and analytical phase shifts plotted as a function of energy for a potential depth of 20 MeV

Once the phase shift is acquired, it is trivial to calculate the total cross section using equation 13. Where the partial wave cross sections can be calculated individually. Again, we show there is agreement between the analytical solution and numerical solution in figure 4.

If we increase the depth of the potential to $V_0 = 60$ MeV we have the formation of a bound state. The plot of phase shifts for this deeper potential can be seen in figure 5. The phase shift at zero energy can be seen to be at π which is in agreement with the Levinson's theorem, which indicates formation of a bound state. The potential in our case satisfies the condition

$$\frac{\pi}{2} = \sqrt{\frac{2m|V_0|R^2}{\hbar^2}} \quad (34)$$

It is the condition that spherical well of depth V_0 possesses a bound state at zero energy. Since an incident particle would like to form a bound state in the potential well, the energy of scattering system is essentially the same as the energy of the bound state. This bound state is not stable, because of the small positive energy, but still it is much higher for the resonance scattering than for non-resonance scattering.

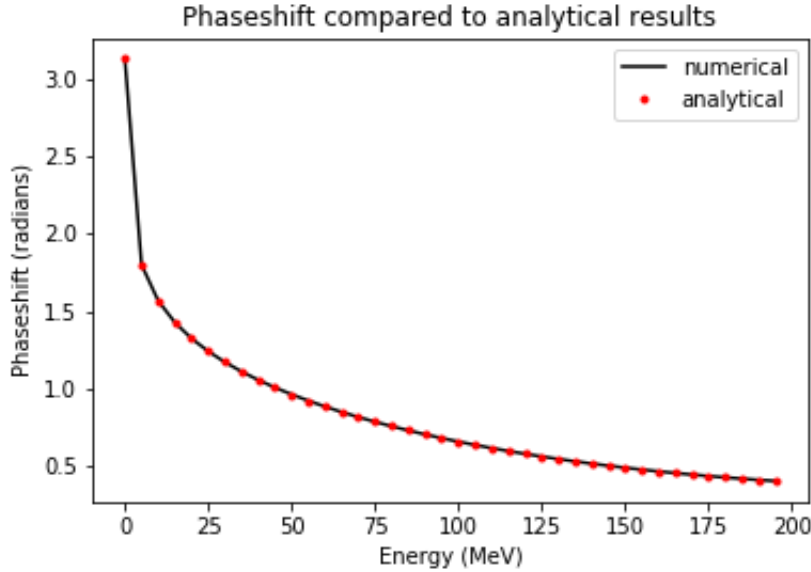


Figure 5: Numerical and analytical phase shifts plotted as a function of energy for a potential depth of 60 MeV

With the calculated partial waves, higher order phase shifts can be examined. The phase shifts for S, P, and D-waves can be seen in figure 6. As expected, as we increase in energy, higher order angular momentum scattering becomes increasingly important. The P and D waves start becoming equally as large at the highest energy of 200. The low energy approximations can also be seen. At energies below 20 MeV, the S-wave phase shift is dominant. This shows that it will be the major contribution to the cross section in scattering.

Once the phase shifts are acquired, acquiring the total cross section is a matter of using equation 13 where we sum over the cross section from each partial wave. The total cross section along with the contributions from each partial wave can be seen in figure 7. The partial wave phase shifts are useful in breaking down which scattering angular momentum states contribute the most to the total cross section. Here we see the same relation as the phase shifts where low energy can be approximated successfully with only the S-wave while higher energies require higher order scattering. Total cross sections are tabulated at a few selected energies in table 1.

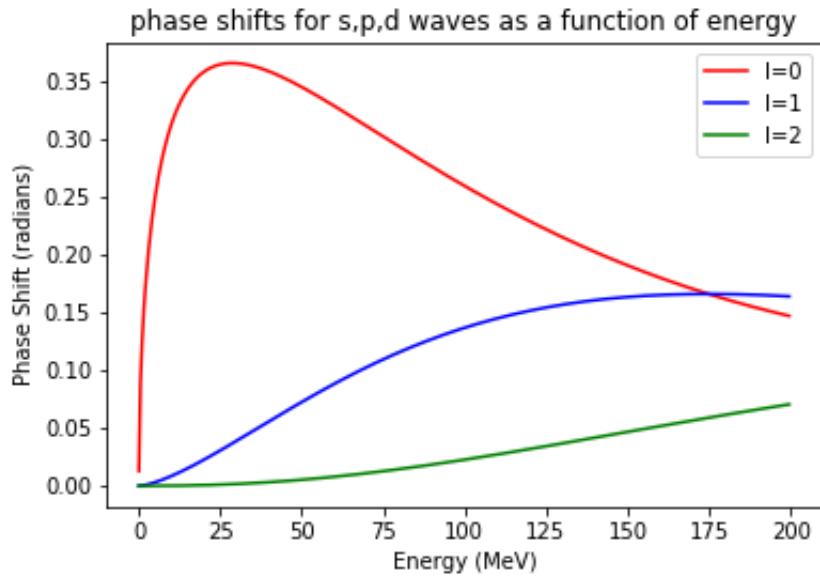


Figure 6: Phase shifts as a function of energy for S, P, and D-wave scattering.

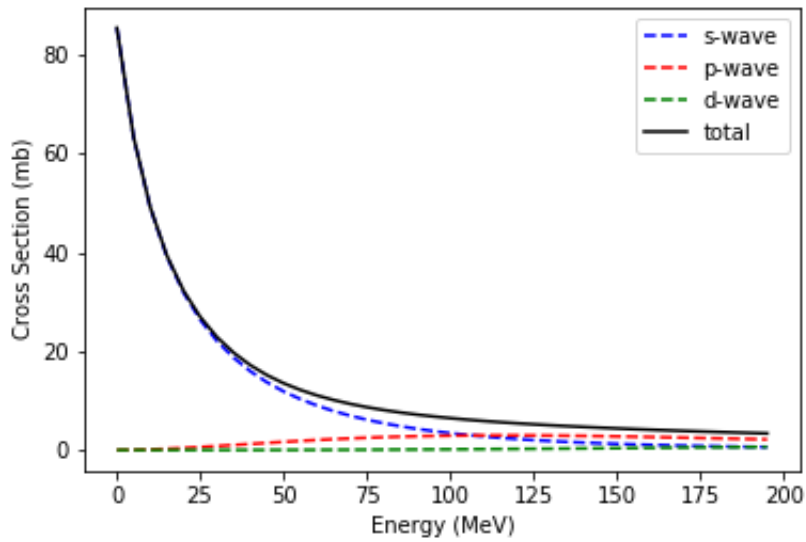


Figure 7: Total cross section as a function of energy

Energy (MeV)	$\sigma_{tot}(mb)$	$\sigma_s(mb)$	$\sigma_p(mb)$	$\sigma_d(mb)$
1	80.6221	80.6208	0.0013	0.0000
10	49.3955	49.2822	0.1132	0.0000
100	6.4529	3.4181	2.9013	0.1335
200	3.2784	0.5552	2.0751	0.6481

Table 1: Cross sections at select energies

4 Conclusions

In this project we described the main concepts of the scattering process. Besides mathematical description of the numerical simulation, we characterized analytical method for the validation of the numerical solution. We used Numerov's method for integrating the radial Schrodinger equation. In addition, we studied methods of deriving total and deferential cross section. From the derivation we learned some essential properties of scattering processes, such as the existence of a partial wave amplitude and a scattering phase causing a phase shift on the outgoing and incoming waves. Python program was used to write the code that can be used to compute partial and total cross section for the different values of V_0, l and m . We successfully applied Levinson's theorem to solve S-wave phase shift discontinuity problem caused by the resonance. Phase shift and cross section plots obtained by the numerical calculations perfectly agree with the data plots obtained by the analytical solution of the problem.

The method presented in this project can be applied to calculate phase shift, partial and total cross section for many different initial parameters. Python program presented here can plot the results, check the solution and successfully resolve resonance problem.